CellPress

Chem

Perspective

Hydrazones as New Molecular Tools

Baihao Shao[1] and Ivan Aprahamian[1,*]

SUMMARY

The development of new classes of molecular switches with enhanced performance and brand-new functionalities enables practitioners to push the frontiers of adaptive and biomimetic materials. The past decade has witnessed the emergence of photo- and chemically activated hydrazones as new molecular tools that can be used in addressing many of the challenges facing the field of molecular switches and machines. In this perspective, we walk through the evolution of these switches and highlight the unique dynamic and/or adaptive capabilities that they bring forth, allowing access to unprecedented opportunities. We focus on reaction cascades driven by the chemically activated switches and show how dynamic intermolecular communication can be used in advancing a systems chemistry approach to solving challenges in the field. As for photochemically activated hydrazones, their bistability enables the multistate actuation of polymers as well as the kinetic trapping of different self-assemblies of liquid crystals, resulting in an emergent phenomenon.

INTRODUCTION

Molecular switches[1] are powerful and effective dynamic tools that confer adaptivity to chemical processes and materials that would otherwise be static, thus enabling scientists to remotely control and modulate the properties and functions of such systems. Photochemically activated switches, such as azobenzenes,[2] diarylethenes,[3] and spiropyrans,[4] and chemically driven (e.g., acid/base and redox) ones, such as catenanes,[5] rotaxanes,[6] and metal coordinated complexes,[7] have been successfully used within the past decade in regulating catalytic activity,[8] hydrophobicity,[9] actuation,[10] rheology,[11] phase properties,[12] conductivity,[13] and bioactivity (e.g., photopharmacology),[14] among other functions. Despite these promising leads, what has been accomplished so far in the field lies mainly under the umbrella of proof of concepts, with minimal breakthroughs making the transition from the laboratory environment into real-world applications. The intrinsic drawbacks of these switchable systems (e.g., complicated synthesis, inadequate and inefficient stability and switching in aqueous media or the solid-state, small geometrical changes, poor switching efficiencies, uncontrolled thermal relaxation rates, and fatigue resistance, and the list goes on) as well as our limited understanding of how to properly integrate them in materials and/or use them in switching cascades are the culprits behind this lag.[15] On the bright side, these hurdles, and the limitations set by the historically prevalent switchable systems, have ensued a renaissance of sorts this past decade in the development of new molecular switches, and the optimization of the properties of prevalent ones, resulting in enhanced properties and novel functionalities. These optimization efforts yielded long-lived tetrafluoro-[16] and heteroaryl-azo switches;[17] visible, red, and even near-infrared light-activated diazocines[18] and azo-BF_2 complexes;[19] multistate switchable phenol-diarylethenes;[20] spiropyrans-based

The Bigger Picture

Challenges and opportunities:

- The chemically activated isomerization around the C=N double bond in hydrazones enables unique switching features, such as dynamic intermolecular communication, that expand the horizons of artificial molecular switches
- The bistability of the photochromic hydrazones allows for the kinetic trapping of different liquid-crystalline self-assemblies resulting in an emergent phenomenon and enables the multistate manipulation of polymer actuators
- New strategies for interfacing molecular switches with bulk materials to enable efficient transfer of molecular-level events into useful macroscopic functions are imperative to make the leap from laboratory curiosity into real-life applications

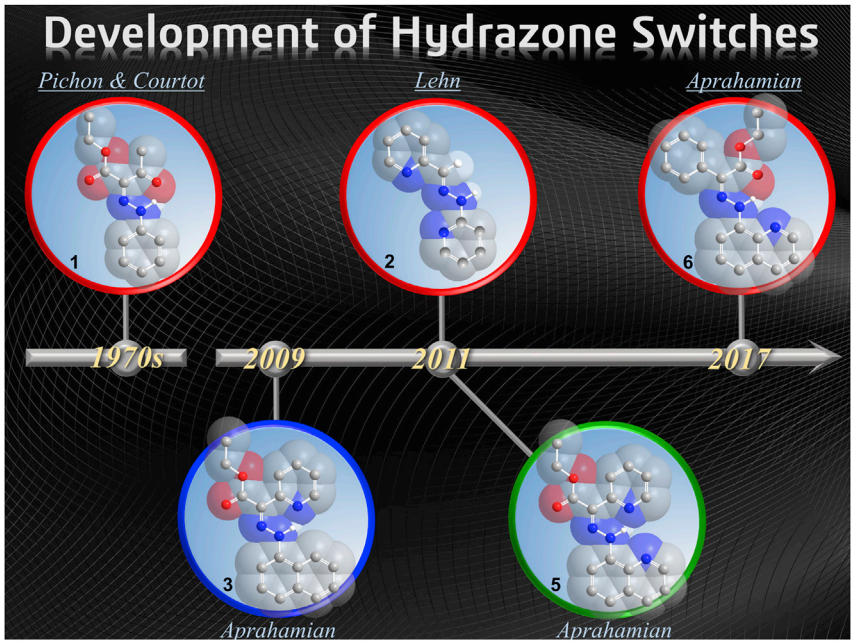

Figure 1. Timeline of the Development of Light (red)-, pH (blue)-, and Zn^{2+}(green)-Activated Hydrazone Switches

photoacids;[21] photoactivable emissive oxazines;[22] chemically activated unidirectional catenane motors;[23] and redox-driven rotaxane pumps,[24] among many other breakthroughs. While new switchable molecular scaffolds, including acylhydrazones,[25,26] imines,[27] indigoids,[28] hemi-indigoids,[29] donor-acceptor Sternhouse adducts,[30] imidazole dimers,[31] dihydroazulenes/vinylheptafulvenes,[32] biphenyl motors,[33] porphyrin spin-state switches,[34] and benzamido-diphenylacetylenes,[35] were recently introduced. These advances attest to the fact that the community has realized that moving the field to the next level will require the drastic expansion and augmentation of the toolbox currently available to practitioners.[36]

In this perspective, we will focus on recently developed chemically and photochemically activatable hydrazone switches[37] while highlighting the new features that they bring forth. To this end, we will focus on select examples from the literature and showcase how this structurally simple scaffold has evolved into an efficient tool for advancing new opportunities and possibilities, while addressing many of the issues bogging down the fields of molecular switches and adaptive materials.

TOOL DEVELOPMENT

One of the key motivations for developing new families of molecular switches is to exploit the novel properties and functions that they enable, thus expanding on the scope of what available tools can perform and allowing for the design of more sophisticated adaptive functional systems. The versatile and multifaceted hydrazone functional group (C=N–NH), with its nucleophilic imine bond and acidic NH proton, has been historically used in synthesis, ion sensing, metal chelation, and dynamic covalent chemistry, among other applications.[38] What was less developed and appreciated though, at least until a decade ago when we entered the scene, was the use of the *Z/E* isomerization around the hydrazone C=N double bond in the development of molecular switches (Figure 1).[37] The reason behind this disparity was the sluggishness of the chemically induced isomerization of such bonds, and a lack of attention

[1]Department of Chemistry, Dartmouth College, Hanover, NH 03755, USA

*Correspondence: ivan.aprahamian@dartmouth.edu

https://doi.org/10.1016/j.chempr.2020.08.007

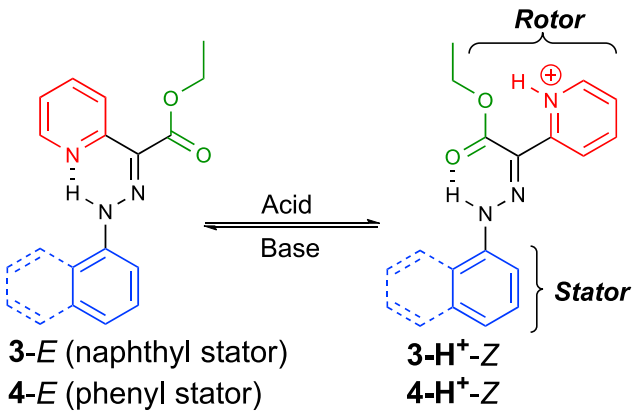

Scheme 1. Switching of Hydrazones 3 and 4 Using Acid and Base

to the research done in the late 70s by Pichon and Courtot on photoswitchable β-ketoester based hydrazones (**1**).[39] These latter studies, and subsequent ones conducted by Lehn and co-workers on hydrazones (**2**),[25] informed us on our quest to develop hydrazones as efficient chemically and/or photochemically activated configurational switches.

Our first foray into hydrazone switches was in 2009, when we reported on the first pH-activated configurational switch **3**.[40] The key structural change that allowed us to convert the sluggish chemically modulated hydrazones into efficient switches was the replacement of the acetyl group in **1** with a pyridyl one. This modification introduced a proton acceptor to the molecule allowing for the quantitative acid-induced switching of **3** between its neutral *E* and protonated *Z* forms (Scheme 1). Deprotonation of **3**-H^+-*Z* with base results in the metastable *Z* isomer, which decays as a function of time to yield the initial *E*-rich solution. In a later iteration and to overcome the limitations set by the use of chemical input in switching, i.e., waste accumulation, we coupled the hydrazone switch **4** with a reversible spiropyran-based photoacid allowing us to cycle the switching process more than 100 times without the accumulation of even a trace amount of waste product.[41] This work highlighted the benefits of dynamic inter-molecular communication (DIMC) and how obstacles in the field of molecular switches can be addressed by coupling different types of molecular switches together.

We explored the idea of DIMC further with hydrazone **5** bearing a quinolinyl instead of a naphthyl stator group (Scheme 2). By itself hydrazone **5** undergoes a highly controllable four-step switching cycle where the configuration and conformation around two axles (i.e., C=N imine bond and N–C_{quin} bond, respectively) can be modulated using acid and base inputs (Scheme 2).[42] When the switching is done using zinc(II) as the input (Scheme 2), then coordination-coupled deprotonation (CCD) takes place resulting in configurational switching and a highly acidic pyridinium proton, which can be used in DIMC. For example, CCD was used in a switching cascade involving proton relay between two different hydrazones[43] and in the reversible manipulation of imine catalysis resulting in signaling as well as signal amplification.[44] These examples showcase how DIMC introduces a systems chemistry[45] approach to the field of molecular switches, allowing for the control over various processes occurring in tandem in solution.

Beyond the use of chemical inputs, we have also been interested in the photoswitching performance of the hydrazones. While hydrazone **4** is a sluggish photoswitch,

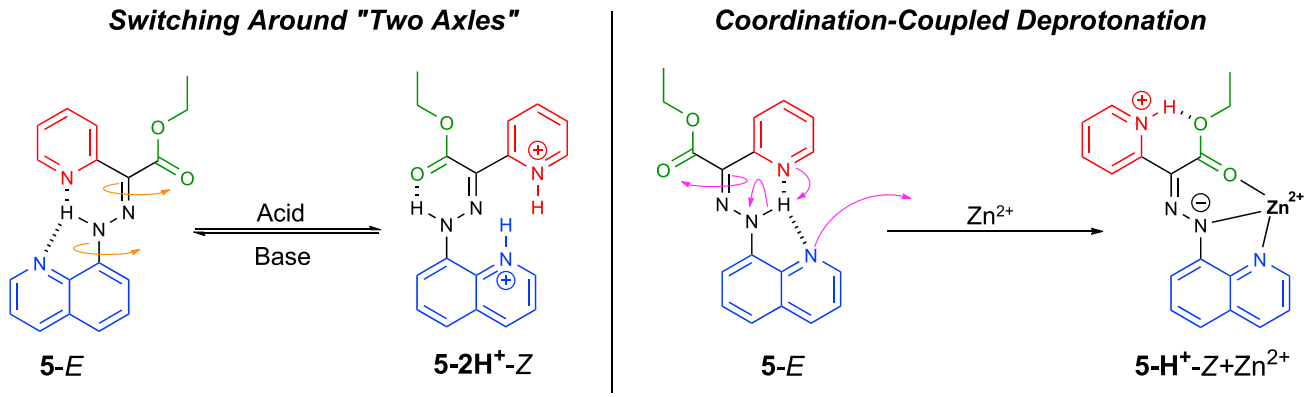

Scheme 2. The Two Characteristic Operating Modes of Hydrazone 5: Switching Around "Two Axles" (Left) and Coordination-Coupled Deprotonation (Right)

hydrazone **5** undergoes an efficient light-induced $E \rightarrow Z$ isomerization with a photostationary state (PSS) of 95% *Z*.[46] However, reminiscent of Lehn's systems (**2**), the $Z \rightarrow E$ isomerization could not be induced photochemically and only occurred thermally with a half-life ($\tau_{1/2}$) of tens of days at room temperature.[25] We hypothesized that the presence of two hydrogen-bond (H-bond) acceptors, i.e., ester and pyridyl, at the rotary fragment of the switch may be the culprit behind the lack of $Z \rightarrow E$ photoisomerization, and hence, we replaced the pyridyl group with a phenyl one and obtained switch **6**.[46] Hydrazone **6**-*Z* can be switched in both directions with light; irradiation with 442 nm light results in a PSS_{442} of 91% *E*, while subsequent 340 nm light irradiation yields a PSS_{340} of 76% *Z* (Scheme 3). This result supports our assumption that the additional intramolecular H-bond in **4** and **5** is responsible for the inefficient and/or photochemically irreversible switching. Interestingly, the removal of the H-bond also results inbistable photoswitchable hydrazones that have half-lives of up to 5,000 years in toluene.[47] Such long thermal half-lives are rare in the context of configurational switches and open the way for using these hydrazone switches in the kinetic trapping of self-assembled structures as we will see later.

SYNTHETIC BIOMIMETIC NEGATIVE FEEDBACK LOOP AND PROGRAMMABLE MOLECULAR ASSEMBLER ENABLED BY QUINOLYL HYDRAZONES

Maintaining homeostasis in living organisms requires the synergy of positive and negative feedback loops,[48] which simplistically can be viewed as sophisticated versions of DIMCs. Developing such synthetic loops, while not trivial, is of general interest to diverse research fields that are beyond the realm of biology, as they can be used in controlling the operation of molecular systems and assemblies that function out of equilibrium, for example.[49] With such opportunities in mind, we decided to design a negative feedback loop based on CCD (Figure 2A).[50] The design principle we used is straightforward—CCD will be used to deprotect a masked aminoquinoline but only when a certain acidic pH level is reached, which will only happen when a certain threshold, which in this case is 20 mol %, of zinc(II) is surpassed. Once these requirements are met, the newly produced amine will condense with an aldehyde, forming an imine ligand that can also coordinate with zinc(II). We designed this imine ligand such that it has a higher binding constant with zinc(II) than the hydrazone, so once the imine is formed it will sequester the metal from **7**-H^+-Z+Zn^{2+}. This process in turn will shift the equilibrium in Figure 2A

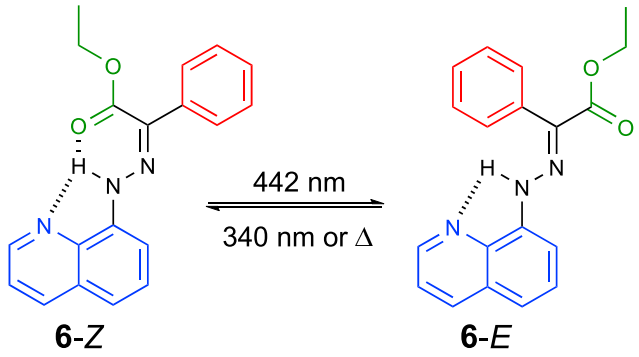

Scheme 3. Light-Activated *Z*/*E* Isomerization of Hydrazone 6

to the left, thus increasing the pH in solution and stopping the deprotection reaction once the excess (i.e., anything above 20 mol %) of zinc(II) is sequestered from the solution. Thus, the signal that starts the cascade of reactions, i.e., excess zinc(II), results in its own demise, which is the basic principle by which negative feedback loops operate. In essence, what we are doing here is using DIMC in buffering both the proton (and hence pH) as well as the zinc(II) concentrations in the solution using a negative feedback loop. This unprecedented example showcases how the careful design of reaction cascades can be used in constructing artificial systems that emulate the hierarchy and interactivity found in biological systems. The next challenge is coupling such a system with a positive feedback loop to design new oscillating systems or using it to regulate complicated dynamic processes that function out of equilibrium, bringing us a step closer to the complexity observed in nature.

The external modulation of multiple rotary motions in the same molecular scaffold, as we demonstrated through switching around the two axles of **5** (Scheme 2),[42] is an important development in the field, as it allows for the controlled spatial movement of different parts of a molecule between various well defined positions. The unique feature of **5** that allows for such a high fidelity in the control over relative molecular motion is that the stator and rotor parts are held in fixed relative orientations through two intramolecular H-bonds. These two parts can be switched around only when adequate amounts of acid and base are added, i.e., there is no free conformational rotation around the axles. The Leigh research group took advantage of this property in their design of a molecular robotic arm that can pick-up, transport, and release a molecular cargo,[51] and of a programmable molecular assembler (**8**) that can be used in asymmetric synthesis.[52] We will focus on the latter system here, which addresses a long-standing goal in organic synthesis—the one-pot control over the stereoselectivity of a reaction outcome. Most switchable catalysts in the literature can only be modulated ON and OFF and cannot be used in the active control over the stereochemistry of a given product.[8] To address this issue with stereoselectivity, Leigh and co-workers incorporated two bulky pyrrolidine catalysts (pink) having different chiralities to opposite sides of the quinolyl stator (**8**).[52] These structural modifications were made so that the swinging of the robotic arm between the two chiral docking stations will result in stereoselective iminium-enamine organocatalysis (Figure 2B). In a nutshell, a protected aldehyde is first loaded to the assembler via olefin metathesis, followed by deprotection to afford an α,β-unsaturated aldehyde substrate (red). An iminium-catalyzed addition of a thiol to this substrate (step 1) generates a mono-substituted saturated aldehyde. Subsequently, the addition of the enamine, formed by condensation of the aldehyde and pyrrolidine, to another electrophile ($H_2C{=}C(SO_2Ph)_2$) gives the disubstituted intermediate, the reduction of

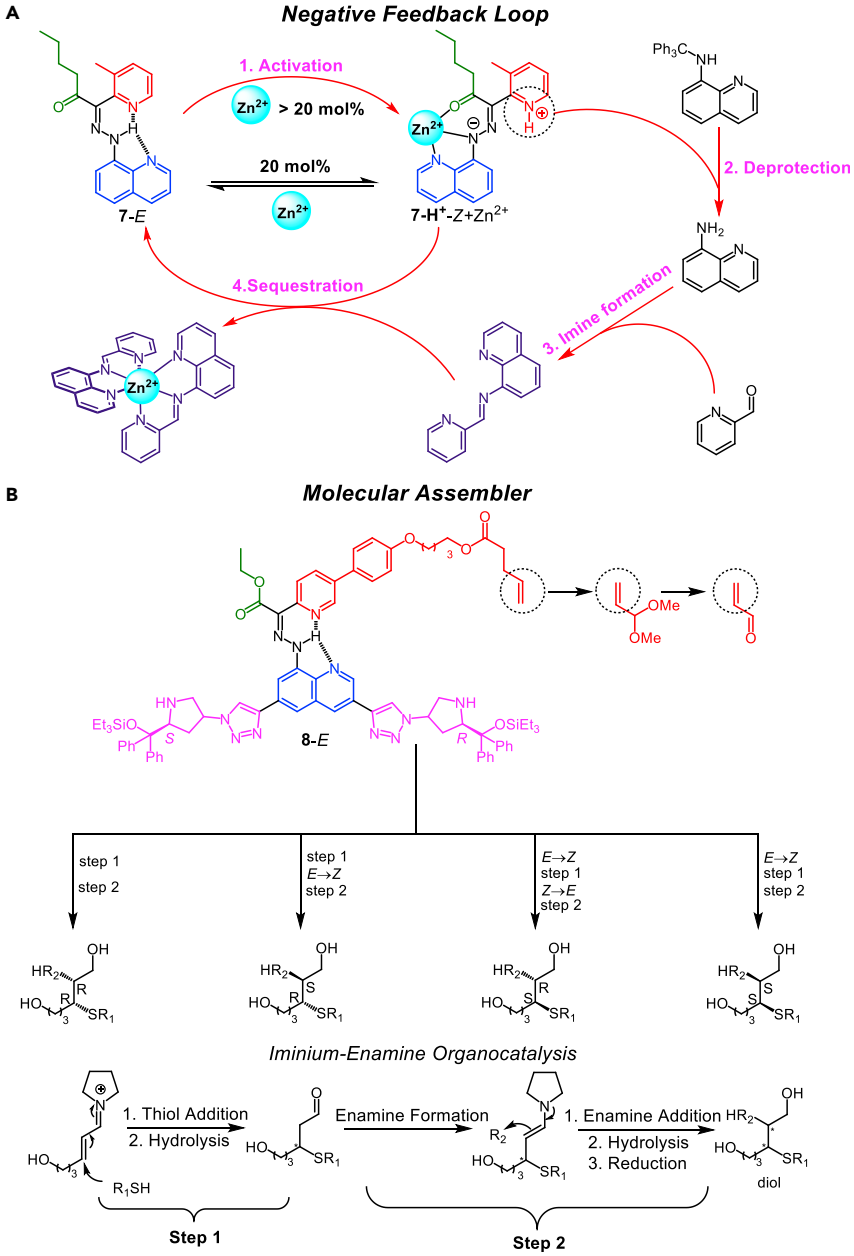

Figure 2. Negative Feedback Loop and Molecular Assembler Based on Hydrazone 5

(A) Dual buffering of pH and zinc(II) concentration using a hydrazone-based negative feedback loop. The process depicted in red arrows starts only when a particular threshold of zinc(II) is surpassed.

(B) Iminium-enamine organocatalysis is used in the stereoselective synthesis of all four diastereoisomers of a diol compound using hydrazone switch **8**.

which leads to the final diol (step 2). The selection of which pyrrolidine catalyst is involved in steps 1 and 2 is governed by the pH-activated *Z/E* isomerization of the hydrazone core. Ultimately, the choice of switching sequence in tandem with iminium-enamine catalyzed reactions generate four diastereoisomers using a single molecular switch. This exquisite control over stereoselectivity gives us a glimpse of the reach and benefits that switchable catalysts bring to the table. This

accomplishment also brings us a step closer to a grand challenge in switchable catalysts—the development of orthogonal systems that can work together in directing multistep stereoselective chemical transformations.

BISTABILITY-ENABLED KINETIC TRAPPING OF SELF-ASSEMBLED STRUCTURES

To further improve on the photophysical properties of hydrazone photoswitch **6**, we conducted structure-property analyses[53] that helped us identify (1) a push-pull bistable hydrazone whose *Z*/*E* isomerization can be triggered solely with visible light, (2) a NMe_2-functionalized hydrazone that exhibits ON and OFF emission toggling and two-photon assisted (i.e., near-infrared activation) $Z \rightarrow E$ isomerization, (3) hydrazones that undergo efficient solid-state *Z*/*E* photoisomerization, (4) a number of switchable solid-state hydrazone emitters, and (5) the underlying principles behind the unusual thermal stability[54] and solid-state emission and switching of the switches. In general, the newly developed switches have very high photoswitching efficiencies, i.e., high PSSs and quantum yields and can be switched in various media—from fetal bovine serum buffer to the solid-state and even on metal surfaces.[55] Here, we want to focus on the unique properties of these switches, especially in the context of configurational switches, namely their bistability and emission toggling.

The large geometrical change that the hydrazones undergo upon *Z*/*E* isomerization can be used in influencing the properties of bulk materials within which they are incorporated. Bistability allows for the locking in of these materials in various non-equilibrated states, i.e., kinetically trapped ones, as a function of *Z*/*E* isomer ratio (i.e., PSS), which can be controlled either by irradiation time or wavelength. The functionalization of the hydrazones with a *para*-NMe_2 substituent brings forth its second unique property, i.e., emission toggling of the hydrazone switch.[56] The isomer ratio-dependent emission in these systems opens the way for the monitoring of photoswitching events as they occur even in the condensed phase using fluorescence microscopy. The combination of all these aforementioned properties, e.g., high efficiency, bistability, switching in various media, and switchable emission, which are all featured in a structurally simple hydrazone scaffold, make the hydrazone photoswitches a very promising addition to the toolbox available to the community.

Multistep and persistent control over the properties of bulk materials and supramolecular assemblies are highly sought-after properties in the context of adaptive functional materials.[57] Attaining such control though is not straightforward using the vast majority of photoswitches in the literature, as in most cases such systems have short thermal half-lives and/or small geometrical changes upon photoisomerization.[2–4] The hydrazone switches on the other hand are well suited for addressing such shortcomings as they undergo large geometrical changes upon isomerization and have thermal half-lives of hundreds to thousands of years. The combination of both these properties can be used in locking structural changes indefinitely, allowing for the development of smart materials that exhibit multilevel and long-lasting functions. We decided to test this hypothesis by using the hydrazone photoswitches in the kinetic trapping of different self-assembled structures as a function of activation wavelength or irradiation time-dependent photostationary states, resulting in composition-dependent (i.e., *Z*/*E* isomer ratios) functions and properties.

We first tested our hypothesis by using the bistable chiral dopant **9** (Figure 3A) in controlling the helical self-assembly and, hence, photophysical properties of liquid

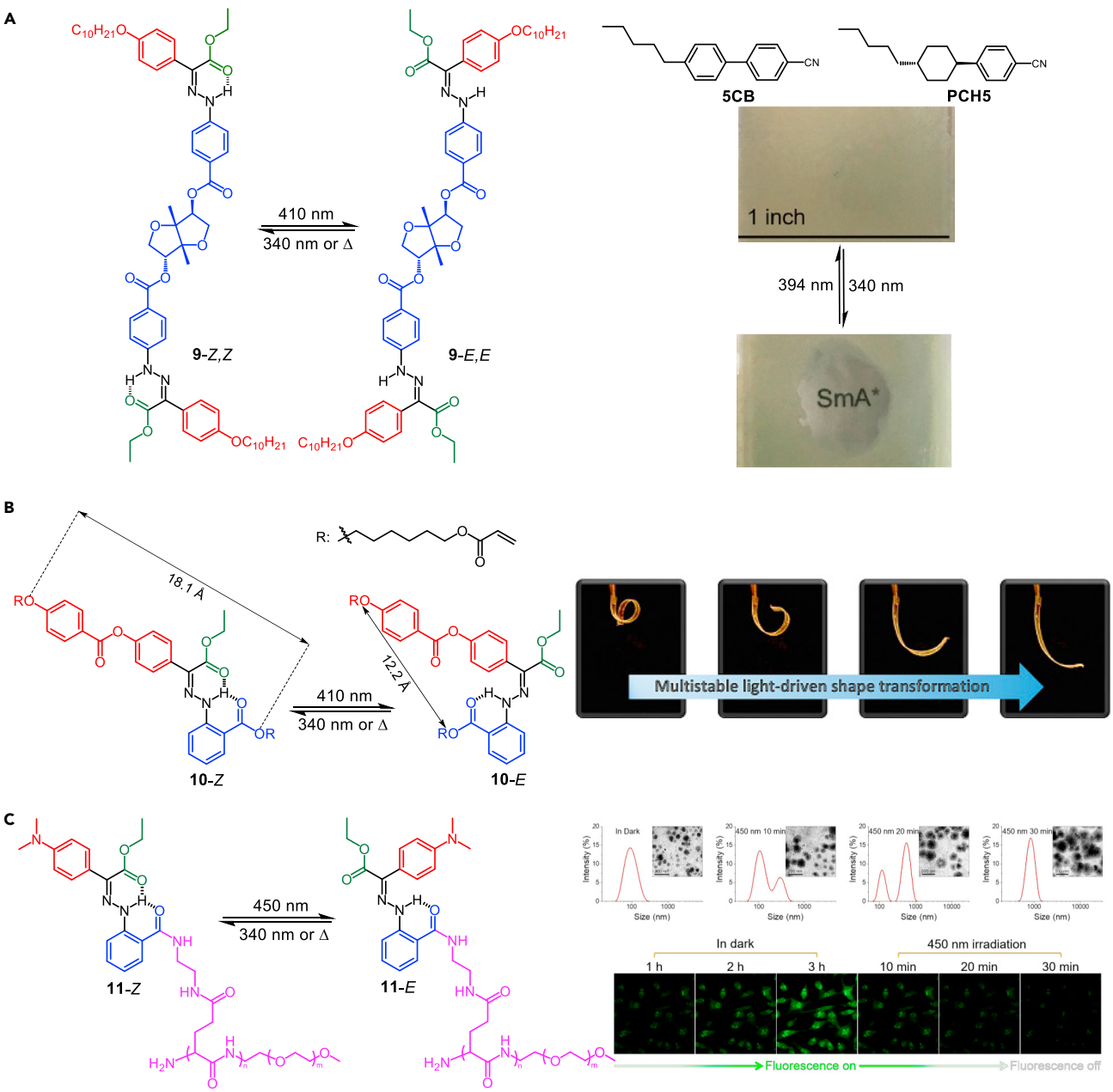

Figure 3. Multistage Modulation of Functions and Properties by Kinetically Trapping Different Supramolecular Assemblies

(A) Light-activated *Z*/*E* isomerization of the hydrazone dopant **9** (left). Structures of nematic LCs 5CB and PCH5 (top right). A light-controllable smart window based on switch **9** (bottom right). Adapted with permission from Moran et al.[58] Copyright 2018 American Chemical Society.

(B) *Z*/*E* photoisomerization of the bifunctional hydrazone monomer **10** (left). The arrows show the contraction in size brought about by hydrazone photoisomerization. Multilevel and persistent actuation of a LC elastomeric film (right). Adapted with permission from Ryabchun et al.[60] Copyright 2019 American Chemical Society.

(C) Light-induced *Z*/*E* switching of the hydrazone-functionalized amphiphilic copolymer **11** (left). Characterization of the irradiation time-dependent nanoparticle expansion using dynamic light scattering and transmission electron microscopy (top right). Demonstration of the cellular uptake of the hydrazone-functionalized nanoparticle and controllable fluorescence emission in MDA-MB-231 cells (bottom right). Adapted with permission from Guo et al.[61] Copyright 2020 Royal Society of Chemistry.

crystals (LCs).[58] The long alkyl chains in **9** were introduced to enhance solubility of the switch in LCs, and a chiral isosorbide linker was used so that the dopant can impart chirality and helicity on the self-assembled LCs. The dopant was then

introduced into commercially available LCs 5CB and PCH5 to yield photoswitchable cholesteric LCs. Switching the dopant using different wavelengths of lights results in PSS-dependent isomer ratios, which can be sustained indefinitely because of the bistability of the dopant. In turn, the different helical pitches that these isomer ratios induce in the LC can be locked-in, resulting in the reflection of different wavelengths of light from the surface of the LC. In essence, the bistability of the dopant is allowing us to kinetically trap different supramolecular self-assemblies of the same LC and, hence, the photophysical properties of the system. For example, in the case of LC 5CB, photoswitching results in the PSS-dependent reflection of different near-infrared wavelengths of light from the surface of the LC. Most interestingly, irradiating 5CB with 394 nm light leads to a transition from a cholesteric to a non-twisted lamellar smectic A* (SmA*) phase. It is very important to note here that 5CB does not inherently yield a SmA* phase, which means that the hydrazone dopant at the isomer ratio that is obtained using 394 nm is resulting in an emergent phenomenon! We currently do not have a concrete explanation as why this is happening, though our working hypothesis is that it results from the unique order-to-order transitions (versus the order-to-disorder transitions that are observed in all other photoswitches)[59] that the hydrazone switches impart on bulk materials upon photoisomerization. To take advantage of the change in LC phase and accompanied change in light transmission properties, we developed a light-controlled smart window (Figure 3A), where photoswitching with 394 and 340 nm lights toggles the LC between an opaque cholesteric phase and a transparent SmA* phase, allowing us to hide and show items placed behind the photoswitchable window. This example is an important illustration of the benefits that can be reaped from configurational bistability, and the unprecedented opportunities that new molecular tools enable.

Next, and to amplify molecular-level photoswitching into a macroscopic motion that can be observed with the naked eye, we, with the help of our collaborators,[60] developed the acrylate-terminated hydrazone monomer **10** and covalently incorporated it into a LC elastomer as a dopant (Figure 3B). As expected, the photoswitching of the obtained polymeric film, resulted in photoactuation. What distinguishes this photoswitchable polymeric actuator from others in the literature[62] is that we can indefinitely lock-in different polymer film shapes by varying the irradiation time (i.e., *Z*/*E* isomer ratio). Such a multistage and multistable polymer actuation has not been demonstrated before, which again attests to the benefit of having a bistable configurational photoswitch. As for the actuation mechanism, we hypothesize that it results from the order-to-order transitions that these switches enforce on bulk materials, which in this case is coupled with a 0.6 nm contraction (Figure 3B) in the size of the dopant upon isomerization, resulting in a mechanical stress on the cross-linked LC polymer. Hence, not only do we have a new functionality and means by which to control bulk materials, but it also occurs through a new molecular-based actuation mechanism.

More recently, we took advantage of the bistability, *Z*/*E* configurational switching, and ON/OFF emission toggling of the hydrazones in developing a traceable drug delivery system. To this end, we attached the NMe_2-functionalized hydrazone to an amphiphilic copolymer (**11**), which was then self-assembled into a core-shell nanostructure (Figure 3C).[61] The emissive hydrazone enabled us to visualize the nanoparticle distribution in cells, and its *Z*/*E* isomerization was then used to trigger drug release from the nanocarriers. The bistability of the hydrazone allowed us to access and lock-in nanoparticles of varying sizes, and when combined with emission toggling, we were able to regulate and even estimate where and how much

drug (i.e., doxorubicin) is being released. We then used this drug delivery mechanism in demonstrating effective light-triggered cytotoxicity in MDA-MB-231 cells. It is important to note here that all these functions were accessible using biocompatible visible light activation. The uniqueness of this system lies in the simplicity by which the hydrazone switch allows for the tracking of the localization of the nanoparticles in cells and then monitoring of where and how much drug is being released. To accomplish these tasks otherwise requires the overcomplication of the drug delivery systems, which in turn can be detrimental to its function by enhancing its cytotoxicity.

CONCLUSION

With this perspective, we showcased the benefits that can be reaped from developing new molecular switches, while highlighting how such tools bring new opportunities to the field of molecular switches and machines in particular and adaptive materials in general. We focused on hydrazones as this is our functional group of choice for addressing the limitations and expanding on the capabilities of the toolset currently available to practitioners. For example, hydrazone switch **5** with its characteristic double H-bond motif ensures high conformational and configurational fidelity, enabling the efficient and precise displacement of chemical cargo within an individual molecule, thus allowing for stereoselective synthesis. On the other hand, CCD enables the development of biomimetic reaction cascades, including a negative feedback loop showcasing how DIMC can contribute to the development of molecular switch-based systems chemistry. In the realm of photoswitches, the bistability of the hydrazones allows for the kinetic trapping of polymer and supramolecular assemblies resulting in multistate actuation and emergent phenomena that are not tractable with other photoswitches. Other traits, including straightforward synthesis, emission toggling, and switching in a broad range of media and phases, will facilitate the future utilizations of hydrazones in super high-resolution imaging,[63] photopharmacology,[14] holographic imaging,[64] and molecular machines,[15] among other applications. All these possibilities, in conjunction with the increased interest and research activity in the field of molecular switches and machines,[65] ensure that the future of hydrazones switches will be bright.

ACKNOWLEDGMENTS

We are grateful to the generous support from the NSF (CHE-1807428).

AUTHOR CONTRIBUTIONS

I.A. and B.S. conceptualized the topics and prepared the manuscript.

REFERENCES

1. B.L. Feringa, and W.R. Browne, eds. (2011). Molecular Switches (Wiley-VCH).
2. Bandara, H.M.D., and Burdette, S.C. (2012). Photoisomerization in different classes of azobenzene. Chem. Soc. Rev. *41*, 1809–1825.
3. Irie, M., Fukaminato, T., Matsuda, K., and Kobatake, S. (2014). Photochromism of diarylethene molecules and crystals: memories, switches, and actuators. Chem. Rev. *114*, 12174–12277.
4. Klajn, R. (2014). Spiropyran-based dynamic materials. Chem. Soc. Rev. *43*, 148–184.
5. Kassem, S., van Leeuwen, T., Lubbe, A.S., Wilson, M.R., Feringa, B.L., and Leigh, D.A. (2017). Artificial molecular motors. Chem. Soc. Rev. *46*, 2592–2621.
6. Baroncini, M., Silvi, S., and Credi, A. (2020). Photo- and redox-driven artificial molecular motors. Chem. Rev. *120*, 200–268.
7. Goswami, A., Saha, S., Biswas, P.K., and Schmittel, M. (2020). (Nano)mechanical motion triggered by metal coordination: from functional devices to networked multicomponent catalytic machinery. Chem. Rev. *120*, 125–199.
8. Blanco, V., Leigh, D.A., and Marcos, V. (2015). Artificial switchable catalysts. Chem. Soc. Rev. *44*, 5341–5370.
9. Berná, J., Leigh, D.A., Lubomska, M., Mendoza, S.M., Pérez, E.M., Rudolf, P., Teobaldi, G., and Zerbetto, F. (2005). Macroscopic transport by synthetic molecular machines. Nat. Mater. *4*, 704–710.
10. Du, G., Moulin, E., Jouault, N., Buhler, E., and Giuseppone, N. (2012). Muscle-like supramolecular polymers: integrated motion from thousands of molecular machines. Angew. Chem. Int. Ed. Engl. *51*, 12504–12508.

11. Lin, Q., Hou, X., and Ke, C. (2017). Ring shuttling controls macroscopic motion in a three-dimensional printed polyrotaxane monolith. Angew. Chem. Int. Ed. Engl. *56*, 4452–4457.

12. Zhou, H., Xue, C., Weis, P., Suzuki, Y., Huang, S., Koynov, K., Auernhammer, G.K., Berger, R., Butt, H.J., and Wu, S. (2017). Photoswitching of glass transition temperatures of azobenzene-containing polymers induces reversible solid-to-liquid transitions. Nat. Chem. *9*, 145–151.

13. Jia, C., Migliore, A., Xin, N., Huang, S., Wang, J., Yang, Q., Wang, S., Chen, H., Wang, D., Feng, B., et al. (2016). Covalently bonded single-molecule junctions with stable and reversible photoswitched conductivity. Science *352*, 1443–1445.

14. Fehrentz, T., Schönberger, M., and Trauner, D. (2011). Optochemical genetics. Angew. Chem. Int. Ed. Engl. *50*, 12156–12182.

15. Aprahamian, I. (2020). The future of molecular machines. ACS Cent. Sci. *6*, 347–358.

16. Bléger, D., Schwarz, J., Brouwer, A.M., and Hecht, S. (2012). o-Fluoroazobenzenes as readily synthesized photoswitches offering nearly quantitative two-way isomerization with visible light. J. Am. Chem. Soc. *134*, 20597–20600.

17. Calbo, J., Weston, C.E., White, A.J., Rzepa, H.S., Contreras-García, J., and Fuchter, M.J. (2017). Tuning azoheteroarene photoswitch performance through heteroaryl design. J. Am. Chem. Soc. *139*, 1261–1274.

18. Lentes, P., Stadler, E., Röhricht, F., Brahms, A., Gröbner, J., Sönnichsen, F.D., Gescheidt, G., and Herges, R. (2019). Nitrogen bridged diazocines: photochromes switching within the near-infrared region with high quantum yields in organic solvents and in water. J. Am. Chem. Soc. *141*, 13592–13600.

19. Yang, Y., Hughes, R.P., and Aprahamian, I. (2014). Near-infrared light activated azo-BF2 switches. J. Am. Chem. Soc. *136*, 13190–13193.

20. Kathan, M., Eisenreich, F., Jurissek, C., Dallmann, A., Gurke, J., and Hecht, S. (2018). Light-driven molecular trap enables bidirectional manipulation of dynamic covalent systems. Nat. Chem. *10*, 1031–1036.

21. Liao, Y. (2017). Design and applications of metastable-state photoacids. Acc. Chem. Res. *50*, 1956–1964.

22. Tang, S., Zhang, Y., Dhakal, P., Ravelo, L., Anderson, C.L., Collins, K.M., and Raymo, F.M. (2018). Photochemical barcodes. J. Am. Chem. Soc. *140*, 4485–4488.

23. Erbas-Cakmak, S., Fielden, S.D.P., Karaca, U., Leigh, D.A., McTernan, C.T., Tetlow, D.J., and Wilson, M.R. (2017). Rotary and linear molecular motors driven by pulses of a chemical fuel. Science *358*, 340–343.

24. Cheng, C., McGonigal, P.R., Schneebeli, S.T., Li, H., Vermeulen, N.A., Ke, C., and Stoddart, J.F. (2015). An artificial molecular pump. Nat. Nanotechnol. *10*, 547–553.

25. Chaur, M.N., Collado, D., and Lehn, J.M. (2011). Configurational and constitutional information storage: multiple dynamics in systems based on pyridyl and acyl hydrazones. Chemistry *17*, 248–258.

26. van Dijken, D.J., Kovaříček, P., Ihrig, S.P., and Hecht, S. (2015). Acylhydrazones as widely tunable photoswitches. J. Am. Chem. Soc. *137*, 14982–14991.

27. Hoorens, M.W.H., Medved', M., Laurent, A.D., Di Donato, M., Fanetti, S., Slappendel, L., Hilbers, M., Feringa, B.L., Jan Buma, W., and Szymanski, W. (2019). Iminothioindoxyl as a molecular photoswitch with 100 nm band separation in the visible range. Nat. Commun. *10*, 2390.

28. Huang, C.Y., Bonasera, A., Hristov, L., Garmshausen, Y., Schmidt, B.M., Jacquemin, D., and Hecht, S. (2017). N,N′-disubstituted indigos as readily available red-light photoswitches with tunable thermal half-lives. J. Am. Chem. Soc. *139*, 15205–15211.

29. Petermayer, C., Thumser, S., Kink, F., Mayer, P., and Dube, H. (2017). Hemiindigo: highly bistable photoswitching at the biooptical window. J. Am. Chem. Soc. *139*, 15060–15067.

30. Lerch, M.M., Szymański, W., and Feringa, B.L. (2018). The (photo)chemistry of Stenhouse photoswitches: guiding principles and system design. Chem. Soc. Rev. *47*, 1910–1937.

31. Mutoh, K., Miyashita, N., Arai, K., and Abe, J. (2019). Turn-on mode fluorescence switch by using negative photochromic imidazole dimer. J. Am. Chem. Soc. *141*, 5650–5654.

32. Broman, S.L., and Nielsen, M.B. (2014). Dihydroazulene: from controlling photochromism to molecular electronics devices. Phys. Chem. Chem. Phys. *16*, 21172–21182.

33. Collins, B.S.L., Kistemaker, J.C.M., Otten, E., and Feringa, B.L. (2016). A chemically powered unidirectional rotary molecular motor based on a palladium redox cycle. Nat. Chem. *8*, 860–866.

34. Köbke, A., Gutzeit, F., Röhricht, F., Schlimm, A., Grunwald, J., Tuczek, F., Studniarek, M., Longo, D., Choueikani, F., Otero, E., et al. (2020). Reversible coordination-induced spin-state switching in complexes on metal surfaces. Nat. Nanotechnol. *15*, 18–21.

35. Jones, I.M., and Hamilton, A.D. (2010). Designed molecular switches: controlling the conformation of Benzamido-diphenylacetylenes. Org. Lett. *12*, 3651–3653.

36. Harris, J.D., Moran, M.J., and Aprahamian, I. (2018). New molecular switch architectures. Proc. Natl. Acad. Sci. USA *115*, 9414–9422.

37. Aprahamian, I. (2017). Hydrazone switches and things in between. Chem. Commun. (Camb.) *53*, 6674–6684.

38. Su, X., and Aprahamian, I. (2014). Hydrazone-based switches, metallo-assemblies and sensors. Chem. Soc. Rev. *43*, 1963–1981.

39. Pichon, R., Le Saint, J., and Courtot, P. (1981). Photoisomerisation d'arylhydrazones-2 de dicetones-1,2 substituees en 2.: mecanisme d'isomerisation thermique de la double liaison C=N. Tetrahedron *37*, 1517–1524.

40. Landge, S.M., and Aprahamian, I. (2009). A pH activated configurational rotary switch: controlling the E/Z isomerization in hydrazones. J. Am. Chem. Soc. *131*, 18269–18271.

41. Tatum, L.A., Foy, J.T., and Aprahamian, I. (2014). Waste management of chemically activated switches: using a photoacid to eliminate accumulation of side products. J. Am. Chem. Soc. *136*, 17438–17441.

42. Su, X., and Aprahamian, I. (2011). Switching around two axles: controlling the configuration and conformation of a hydrazone-based switch. Org. Lett. *13*, 30–33.

43. Ray, D., Foy, J.T., Hughes, R.P., and Aprahamian, I. (2012). A switching cascade of hydrazone-based rotary switches through coordination-coupled proton relays. Nat. Chem. *4*, 757–762.

44. Foy, J.T., Ray, D., and Aprahamian, I. (2015). Regulating signal enhancement with coordination-coupled deprotonation of a hydrazone switch. Chem. Sci. *6*, 209–213.

45. Ashkenasy, G., Hermans, T.M., Otto, S., and Taylor, A.F. (2017). Systems chemistry. Chem. Soc. Rev. *46*, 2543–2554.

46. Qian, H., Pramanik, S., and Aprahamian, I. (2017). Photochromic hydrazone switches with extremely long thermal half-lives. J. Am. Chem. Soc. *139*, 9140–9143.

47. Li, Q., Qian, H., Shao, B., Hughes, R.P., and Aprahamian, I. (2018). Building strain with large macrocycles and using it to tune the thermal half-lives of hydrazone photochromes. J. Am. Chem. Soc. *140*, 11829–11835.

48. A.C. Guyton, and J.E. Hall, eds. (2000). Textbook of Medical Physiology, Eleventh Edition (Elsevier Inc.).

49. Grzybowski, B.A., Wilmer, C.E., Kim, J.B., Browne, K.P., and Bishop, K.J.M. (2009). Self-assembly: from crystals to cells. Soft Matter *5*, 1110–1128.

50. Pramanik, S., and Aprahamian, I. (2016). Hydrazone switch-based negative feedback loop. J. Am. Chem. Soc. *138*, 15142–15145.

51. Kassem, S., Lee, A.T., Leigh, D.A., Markevicius, A., and Solá, J. (2016). Pick-up, transport and release of a molecular cargo using a small-molecule robotic arm. Nat. Chem. *8*, 138–143.

52. Kassem, S., Lee, A.T.L., Leigh, D.A., Marcos, V., Palmer, L.I., and Pisano, S. (2017). Stereodivergent synthesis with a programmable molecular machine. Nature *549*, 374–378.

53. Shao, B., Qian, H., Li, Q., and Aprahamian, I. (2019). Structure property analysis of the solution and solid-state properties of bistable photochromic hydrazones. J. Am. Chem. Soc. *141*, 8364–8371.

54. Shao, B., and Aprahamian, I. (2020). Planarization-induced activation wavelength red-shift and thermal half-life acceleration in hydrazone photoswitches. ChemistryOpen *9*, 191–194.

55. Zheng, L.Q., Yang, S., Lan, J., Gyr, L., Goubert, G., Qian, H., Aprahamian, I., and Zenobi, R. (2019). Solution phase and surface photoisomerization of a hydrazone switch with

a long thermal half-life. J. Am. Chem. Soc. *141*, 17637–17645.

56. Shao, B., Baroncini, M., Qian, H., Bussotti, L., Di Donato, M., Credi, A., and Aprahamian, I. (2018). Solution and solid-state emission toggling of a photochromic hydrazone. J. Am. Chem. Soc. *140*, 12323–12327.

57. Morone, M.I.F. (2018). Harnessing the power of shape shifting polymers. Chem. Eng. News *96*, 36–42.

58. Moran, M.J., Magrini, M., Walba, D.M., and Aprahamian, I. (2018). Driving a liquid crystal phase transition using a photochromic hydrazone. J. Am. Chem. Soc. *140*, 13623–13627.

59. Bisoyi, H.K., and Li, Q. (2016). Light-driven liquid crystalline materials: from photo-induced phase transitions and property modulations to applications. Chem. Rev. *116*, 15089–15166.

60. Ryabchun, A., Li, Q., Lancia, F., Aprahamian, I., and Katsonis, N. (2019). Shape-persistent actuators from hydrazone photoswitches. J. Am. Chem. Soc. *141*, 1196–1200.

61. Guo, X., Shao, B., Zhou, S., Aprahamian, I., and Chen, Z. (2020). Visualizing intracellular particles and precise control of drug release using an emissive hydrazone photochrome. Chem. Sci. *11*, 3016–3021.

62. Lancia, F., Ryabchun, A., and Katsonis, N. (2019). Life-like motion driven by artificial molecular machines. Nat. Rev. Chem. *3*, 536–551.

63. Sahl, S.J., Hell, S.W., and Jakobs, S. (2017). Fluorescence nanoscopy in cell biology. Nat. Rev. Mol. Cell Biol. *18*, 685–701.

64. Poon, T.-C. (2006). Digital Holography and Tree-Dimensional Display: Principles and Applications (Springer Science & Business Media).

65. Iino, R., Kinbara, K., and Bryant, Z. (2020). Introduction: molecular motors. Chem. Rev. *120*, 1–4.